



**HAL**  
open science

## Battery Pack Thermal Modeling, Simulation and Electric Model Identification

Khadija Saqli, Houda Bouchareb, Nacer Kouider M'Sirdi, Mohammed Oudghiri

► **To cite this version:**

Khadija Saqli, Houda Bouchareb, Nacer Kouider M'Sirdi, Mohammed Oudghiri. Battery Pack Thermal Modeling, Simulation and Electric Model Identification. IRSEC 21 – 2021 9th International Renewable and Sustainable Energy, Nov 2021, Rabat (virtual), Morocco. hal-03543211

**HAL Id: hal-03543211**

**<https://hal.science/hal-03543211>**

Submitted on 25 Jan 2022

**HAL** is a multi-disciplinary open access archive for the deposit and dissemination of scientific research documents, whether they are published or not. The documents may come from teaching and research institutions in France or abroad, or from public or private research centers.

L'archive ouverte pluridisciplinaire **HAL**, est destinée au dépôt et à la diffusion de documents scientifiques de niveau recherche, publiés ou non, émanant des établissements d'enseignement et de recherche français ou étrangers, des laboratoires publics ou privés.

# Battery Pack Thermal Modeling, Simulation and Electric Model Identification

Khadija Saqli

LISAC, Sidi Mohamed Ben Abdellah University  
Fez, Morocco  
khadija.saqli@usmba.ac.ma

Nacer Kouider M'sirdi

LIS, Aix Marseille University  
Marseille, France  
nacer.msirdi@lis-lab.fr

Houda Bouchareb

LISAC, Sidi Mohamed Ben Abdellah University  
Fez, Morocco  
houda.bouchareb@usmba.ac.ma

Mohammed Oudghiri

LISAC, Sidi Mohamed Ben Abdellah University  
Fez, Morocco  
oudghiri.ensafes@gmail.com

**Abstract**—Li-ion batteries are susceptible to high and low temperatures. Therefore, thermal management and heat prediction are essential to keep the temperatures of the energy storage system cells inside the optimal range of operation and assure safe and effective usage.

In this paper, an electrochemical-thermal battery pack of three parallel-connected cylindrical Li-ion cells is modelled using COMSOL Multiphysics software. To investigate the impact of the inlet velocity on the evolution of the pack temperature and identify the ideal value capable of maintaining the overall temperature of the battery pack within limits, we placed our cells in a compartment where air flows at different values fixed at the beginning of each simulation.

The developed thermal model was discharged using pulse data current at different temperatures to generate the essential data needed to model an electric-thermal model and identify its parameters in Matlab/Simulink software.

**Index Terms**—Li-ion battery, battery thermal management system, air-cooling, electrochemical-thermal model, equivalent circuit model, parameters estimation, model identification

## I. INTRODUCTION

Numerous research and scientific studies have been conducted for the sake of developing safe and lasting batteries with higher power and energy density [1]. The evolution of energy storage systems has led to the development of Lithium-ion batteries. It has become the most dominant technology nowadays, especially in the electric vehicle market, owing its popularity to its high energy and power density, long life cycle, and no memory effect [2].

Generally, Li-ion batteries are stuck together in series and/or parallel to build an energy storage system with the desired voltage and capacity. During operation, the assembly of many cells in a single compartment induces a temperature increase of the pack, which leads to local deterioration or even explosion if not managed [3]. Li-ion batteries have a temperature optimal operation range of 15°C to 35°C for safe usage [4]. Hence, a thermal management system is essential to dissipate excessive heat and ensure even temperature distribution inside the pack

Battery state of charge(SOC), ambient temperature and ap-

plied current are the key factors that impact the heat generation during operation [5]. Different battery thermal management systems(BTMS) were introduced in the literature. Naixing Yang et al. [6] studied the connection between the design of the battery pack system and the cooling system. G. Karimi and X. Li [7] investigated the impact of cooling conditions and pack configuration on the thermal behaviour of the battery. Dafen Chen et al. [8] compared different cooling approaches, including air-cooling, direct liquid cooling, indirect-liquid cooling and fin cooling. The author deduced that the indirect liquid cooling system has the lowest maximum temperature rise among other cooling approaches.

In [9] H. Park opted to forced air cooling approaches to satisfy the required thermal specifications of HEVs. The author demonstrates that cooling efficiency can be achieved even without changing the design of the existing battery system by using the tapered manifold and pressure relief ventilation.

Air cooling, liquid cooling and phase changing material cooling methods are the primary cooling approach used to mitigate the heat and ensure a uniform temperature distribution [10]. Each of these methods has its advantages and drawbacks regarding efficiency and cost.

Forced air cooling is especially preferred for parallel-connected cells. It's known as the most efficient and straightforward compared to other methods [4].

On the other hand, liquid cooling can dissipate the generated heat with relatively low flow rates. Be that as it may, the complexity, the high cost and the potential leakage of this cooling approach restrain its usage. Finally, phase-change cooling is a cooling method that reduces the pack temperature by changing its secular state from solid to liquid. One major drawback of this method is its inability to eject the absorbed heat, thing that makes it unsuitable for EV application [11].

In this paper, a battery thermal management system is designed to dissipate the generated heat of the three parallel-connected cells using the air-cooling approach. The developed method was then simulated at three different temperatures to extract the necessary data and build an advanced electro-

thermal battery model.

The paper is structured as follow: Section 2 outlines the primary battery models presented in the literature and introduces the developed BTMS. Section 3 presents the parameter identification process of the electro-thermal battery model. Finally, section 4 concludes the work presented in this paper and perspectives for future research.

## II. BATTERY MODELING

Modelling is a crucial phase that allows a better understanding of the underlying process of the battery. Different battery models with various complexity levels and accuracy were presented in the literature. They can be classified into two main categories: equivalent circuit battery models and electrochemical battery models. Equivalent circuit battery models (ECM) uses a set of electrical components to represent the dynamic behaviour of the battery during charge/discharge while neglecting the underlying electrochemical reactions. They are widely reputed for their simplicity, and reasonable accuracy [12]. Generally, ECMs comprise an ideal voltage source, a series with resistance representing the instantaneous voltage drop and one or multiple R-C pairs defining the dynamic response of the battery.

In contrast, electrochemical battery models use physical laws such as Ohm's law, Butler-Volmer law and Fick's law of diffusion to represent the inner chemical reactions that occur inside the battery during charge/discharge [13]. The first electrochemical battery model was introduced by Doyle and Newman [14], [15]. The model shares its name with its developer and uses Maxwell-Stefan equations to describe the ions transport in the electrolyte. Despite its high accuracy, this battery model category is not suitable for real-time applications due to its complexity and high computational cost.

An alternative way of using this type of models is by converting the Partial Differential Equations (PDEs) into Ordinary Differential Equations (ODEs) using methods such as finite element and finite difference methods to discretize the nonlinear PDEs [16].

### A. Comsol Simulation Model

The designed battery pack used in this study is illustrated in Fig. 1. The model comprises 1s3p LMO 18650 cells with a graphite anode linked by small aluminium strips, arranged to create air turbulence, and placed in a compartment where air flows.

Using Comsol Multiphysics software, the Pseudo two-dimensional (P2D) model was developed in two phases: a 1D model representing the cell chemistry using Batteries and Fuel Cells library (see Fig. 2), and a 3D model that describes the evolution of temperature and the cooling airflow using Heat Transfer in Solids and Fluids (Fig. 3).

The 1D cell model comprises a negative porous electrode, separator and positive porous electrode. For each segment, the P2D model solves for the conservation of charge, mass and energy to calculate the lithium concentration in the solid  $c_s$  and in the electrolyte  $c_e$ , the electrolyte and solid potential symbolised respectively as  $\phi_s$ , and  $\phi_e$  plus volumetric reaction current  $J$ .

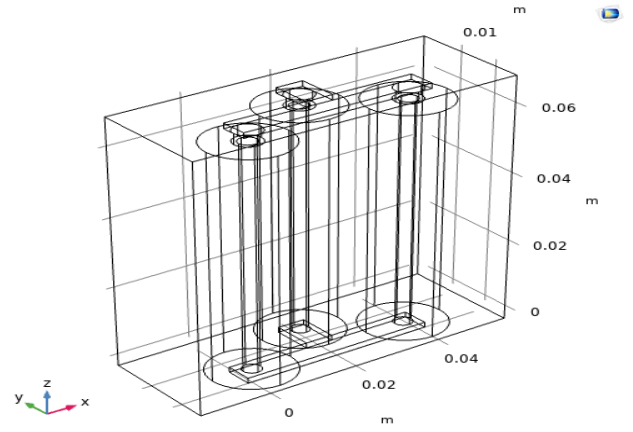


Fig. 1. Battery pack geometry

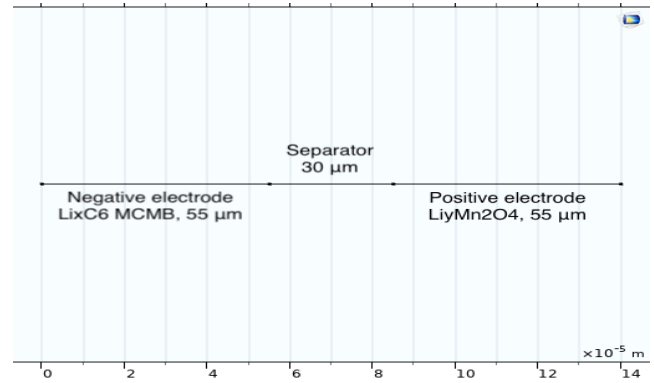


Fig. 2. 1D Li-ion cell geometry

Table 1 summarizes the governing equations and boundary conditions of the electrochemical model. A coupling function for the average temperature in the active battery material and the average generated heat is used to couple the 1D and the 3D model. A succession charge and discharge current pulses with a cycle time of 600s was applied to the battery pack to test the performance of the thermal management system. The initial temperature was set at 25°C and the inlet velocity at 6 m/s.

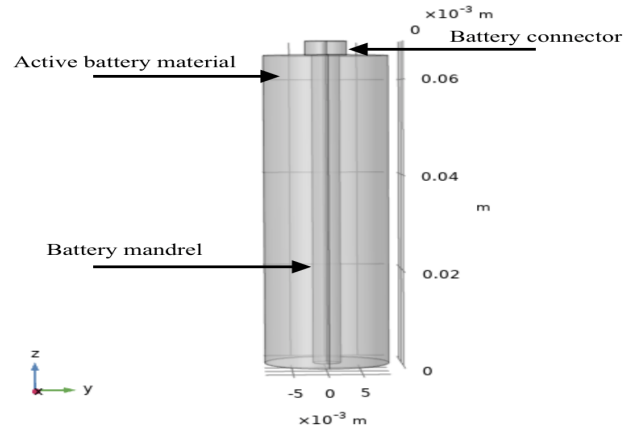


Fig. 3. 3D Li-ion cell geometry

As discussed in the previous section, Li-ion batteries are sensitive to elevated temperatures. The generated heat increases the cell temperature above the permissible limits, leading to thermal runaway if not managed. The heat generation of each cell can be computed using the following equation:

$$\begin{cases} \frac{\partial \rho C_p T}{\partial t} - \nabla \cdot (k \nabla T) = Q \\ Q = \sigma_{eff,p} \nabla^2 \phi_{s,p} + \sigma_{eff,n} \nabla^2 \phi_{s,n} + J [U - (\phi_{s,p} - \phi_{s,n}) - T \frac{dU}{dT}] \end{cases} \quad (1)$$

Where  $C_p$ ,  $T$ ,  $k$ ,  $Q$  and  $U$  represent respectively the heat capacity, the temperature, the thermal conductive coefficient, the generated heat and the battery open circuit voltage.

Fig. 4 illustrates the temperature distribution inside the battery pack at time = 600s. As shown in the figure, the flowing air inside the compartment gets warmer as it moves due to the heat generated by the cells. Thus, the cell placed at the outlet has higher temperatures than the one placed at the inlet.

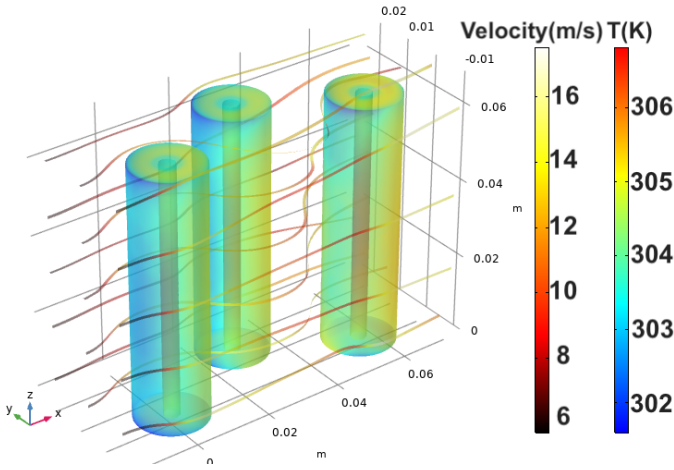


Fig. 4. Temperature distribution inside the battery pack and air cooling flow

Fig. 5 illustrates the evolution of the average temperature of the three cells. During Operation, the generated heat from the redox electrochemical reactions causes the battery temperature to rise.

The temperature of the third cell placed at the outflow is higher compared to the others, which can be explained by the rise of the air temperature.

The voltage variation of each cell during operation is illustrated in Fig. 10. It can be seen that the third cell, which has the highest average temperature, exhibits a slightly higher discharge voltage compared to other cells, which can be explained by the electrical conductivity and lithium diffusion drop with temperature increase.

To study the influence of inlet velocity on battery temperature, we simulated the BTMS at three different inlet velocities: 0.1 m/s, 1m/s and 6 m/s. The simulation results are shown in Fig. 9. An inlet velocity of 0.1m/s was insufficient. The average temperature attained a value of 321K, which highly surpass the maximum limit for safe operation. In comparison, an inlet velocity of 6m/s could satisfy the operation condition that guarantees better execution.

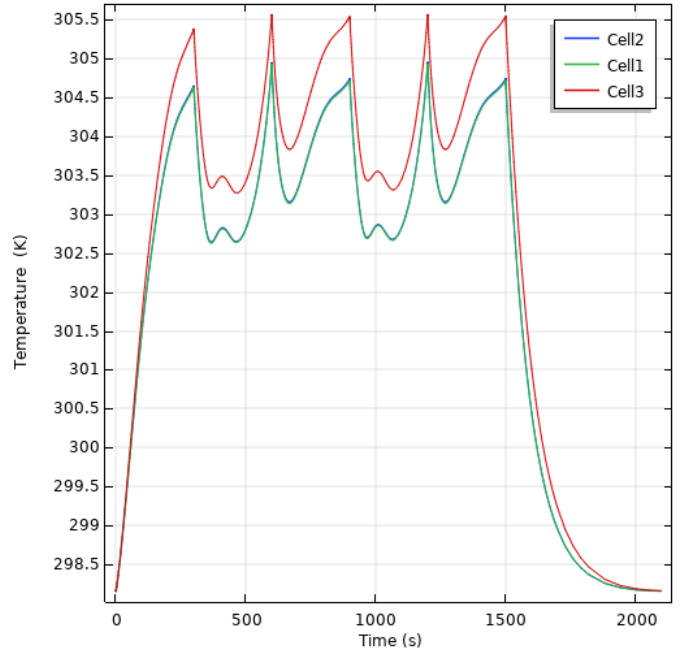


Fig. 5. Average cell temperatures vs time

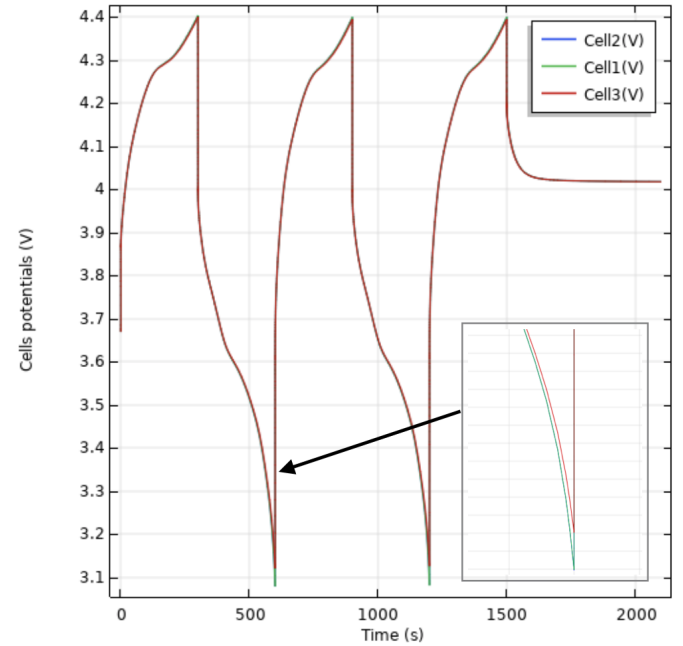


Fig. 6. Cell voltages vs time

III. IDENTIFICATION OF AN EQUIVALENT BATTERY MODEL  
ECMs have been widely used in EV studies thanks to their simplicity and efficiency. Parameter identification is a crucial phase upon which rely the accuracy of the developed algorithms. Determining the battery parameters can be done using impedance spectroscopy and pulse tests. However, these methods rely on specific equipment to test and process many data, making them inconvenient for online applications [17].

TABLE I  
MODEL EQUATIONS AND BOUNDARY CONDITIONS OF THE P2D MODEL.

Description	Governing equations	Boundary conditions
Diffusion inside the solid	$\frac{\partial c_s}{\partial t} = \frac{D_s}{r^2} \frac{\partial}{\partial r} \left[ r^2 \frac{\partial c_s}{\partial r} \right]$	$-D_s \frac{\partial c_s}{\partial r} \Big _{r=0} = 0, -D_s \frac{\partial c_s}{\partial r} \Big _{r=R_p} = j_k$
Lithium concentration in the electrolyte	$\epsilon_k \frac{\partial c_{e,k}}{\partial t}(x,t) = \nabla (D_{eff} \nabla c_e) + a_k(1-t_+)j$	$-D_{eff,p} \frac{\partial c_{e,p}}{\partial x} \Big _{x=0} = -D_{eff,n} \frac{\partial c_{e,n}}{\partial x} \Big _{x=L} = 0$
Potential in the solid phase	$\nabla (\sigma_{eff} \nabla \phi_{s,k}) = a_k F j_k$	$-\sigma_{eff,p} \nabla \phi_{s,p} \Big _{x=0} = 0$ $-\sigma_{eff,n} \nabla \phi_{s,n} \Big _{x=L} = I$ $-\sigma_{eff,p} \nabla \phi_{s,p} \Big _{x=L_p} = -\sigma_{eff,n} \nabla \phi_{s,n} \Big _{x=L_p+L_{sep}} = 0$
Potential in the electrolyte phase	$-\nabla (\sigma_{eff,k} \nabla \phi_e) + \frac{2RT}{F} (1-t_+) \nabla (k_{eff,k} \nabla \ln c_e) + J = 0$	$\frac{\partial \phi_e}{\partial x} \Big _{x=L_n} = 0$ $\frac{\partial \phi_e}{\partial x} \Big _{x=L_p} = 0$
Pore wall flux	$j_k = (c_{s,k,max} - c_{s,k,surf})^{0.5} (c_{s,k,surf})^{0.5} k_k c_{e,k}^{0.5} \left[ \exp\left(\frac{0.5F}{RT} \eta_k\right) - \exp\left(-\frac{0.5F}{RT} \eta_k\right) \right]$	
overpotential of the intercalation reaction	$\eta_k = \phi_{s,k} - \phi_{e,k} - U_k$	

Thus, least-square algorithms and adaptive filtering were used to allow online estimation of the battery parameters [18].

In this study a first-order equivalent circuit model with one RC block was chosen for its simplicity and accuracy [8]. The model includes an open-circuit voltage (OCV) linked in series with an ohmic resistance  $R_0$  and one RC block to model the battery polarisation caused by diffusion and transfer.

The characteristics of this model are presented using the following equations :

$$\frac{dI_1(t)}{dt} = -\frac{1}{R_1 C_1} I_1(t) + \frac{1}{R_1 C_1} I(t) \quad (2)$$

$$\frac{dSOC(t)}{dt} = -\frac{\eta(t)}{Q} I(t) \quad (3)$$

$$U_t = OCV(SOC(t)) - R_0 I(t) - R_1 I_1(t) \quad (4)$$

Where  $I(t)$  and  $I_1(t)$  denote respectively the current across the ohmic resistance  $R_0$  and  $R_1$ , SOC is the battery state of charge,  $\eta$  is the coulomb efficiency used to compensate the loss of charge and  $Q$  is the battery capacity.

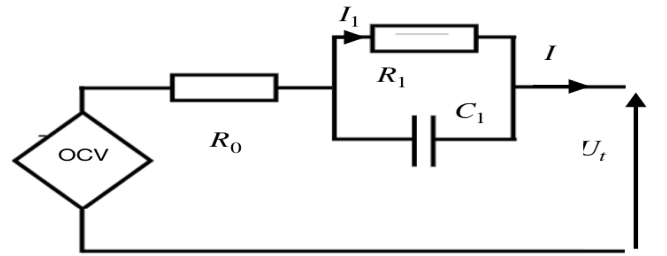


Fig. 8. First-order equivalent circuit model

To build an electro-thermal Li-ion cell model that considers the impact of the battery SOC and ambient temperature on the model parameters. The previously presented electrochemical-thermal model was simulated using successions of discharge pulses of 30 s, each followed by a relaxation period of 120 s at three different temperatures (15 °C, 25 °C, 40 °C).

Each model component was adapted to account for battery SOC and temperature using Simscape blocks and Simscape language, and we used a nonlinear least square approach

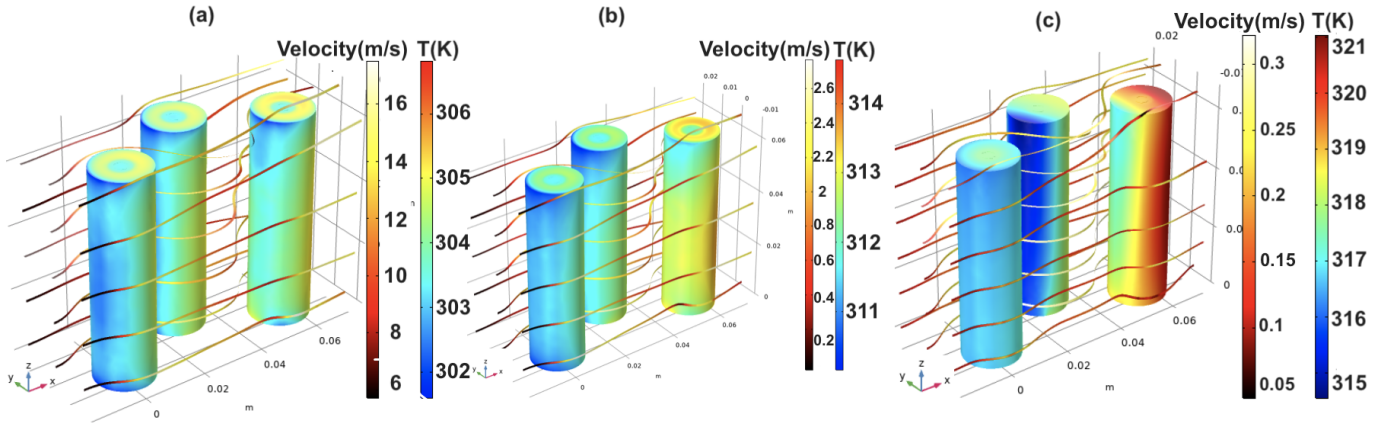


Fig. 7. Temperature distribution in the pack with (a):inlet velocity set at 6 m/s, (b):inlet velocity set at 1 m/s, (c):inlet velocity set at 0.1 m/s.

to predict the value of each parameter at the corresponding SOC and temperature. Fig. 9 illustrates the identified model parameters. The algorithm estimates also the gradient error of each component to identify the best fit function that minimizes the sum of squares errors.

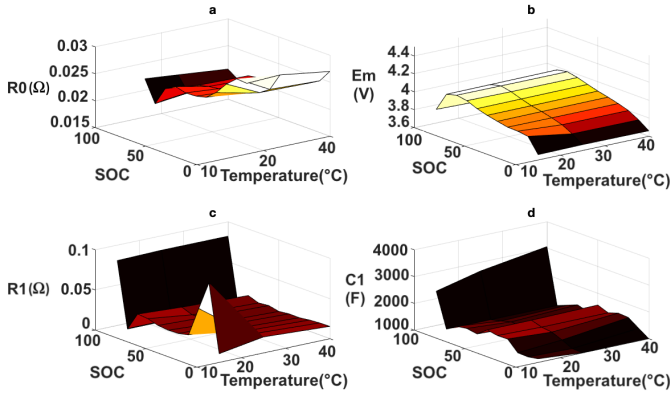


Fig. 9. Battery model parameters (a) Ohmic resistance ,(b) Open circuit voltage, (c) is polar resistance and (c) is the capacitance

The battery SOC was estimated using Coulomb counting approach:

$$SOC(t) = SOC(t_0) - \frac{1}{Q_{rated}} \int_{t_0}^t \eta(t) I_{bat} dt \quad (5)$$

Where  $SOC(t_0)$ ,  $Q_{rated}$  and  $I_{bat}$  represent respectively the initial SOC, the rated capacity and the battery current.

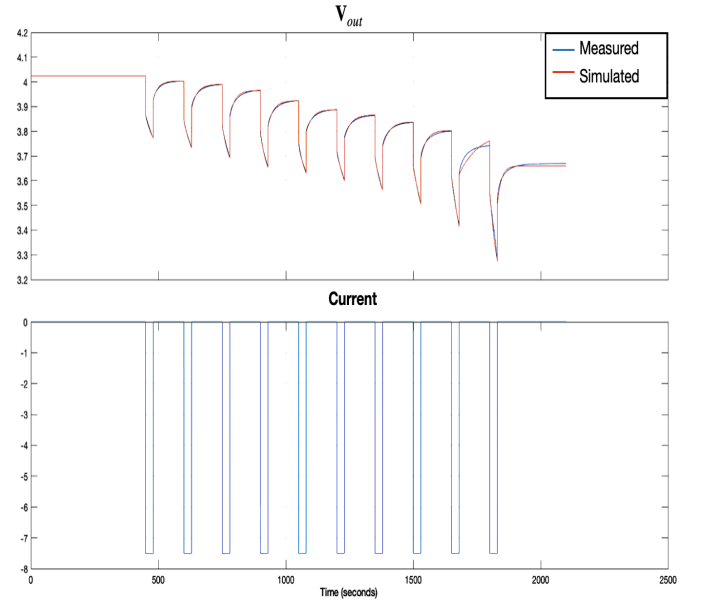


Fig. 10. Battery model parameters (a) Ohmic resistance ,(b) Open circuit voltage, (c) is polar resistance and (c) is the capacitance

Fig. 10 illustrates the agreement between the measured output voltage and the simulated output voltage of the equivalent circuit model at 15 °C.

At the end of the simulation, the relative sum square error changes by  $6.77e-05$ , which shows the ability of the developed equivalent circuit model to emulate with accuracy the battery response during operation.

#### IV. CONCLUSION

In this paper, a battery thermal management system was designed and investigated. The system uses an air-cooling approach to mitigate the heat generated inside a 1s3p LMO 18650 Li-ion battery pack. First, a 3D electrochemical-thermal model that describes the battery pack's thermal behaviour, including airflow, was developed in COMSOL Multiphysics software. The impact of the air inlet velocity and the cell arrangement inside the pack was also investigated. The de-

veloped BTMS was tested by successively charging and discharging the battery pack at 7.5C-rate. Finally, we used the developed system to build an electro-thermal battery model in Matlab software.

The model can be further improved to account for battery hysteresis and other ageing factors that affect the performance, to be able to identify the battery states such as the battery state of charge(SOC) and state of health(SOH).

#### ACKNOWLEDGMENT

The authors and the SASV research group would like to thank the French Embassy in Rabat for their support to the two doctoral students of USMBA for their trip to the LiS lab of Aix Marseille University in 2019.

#### REFERENCES

- [1] R. Kumar and T. Sarakonsri, *High Energy Density Lithium Batteries: Materials, Engineering, Applications*. Wiley-VCH, 04 2010, vol. 53, pp. 53–80.
- [2] C. Iclodean, B. Varga, N. Burnete, D. Cimerdean, and B. Jurchiş, “Comparison of different battery types for electric vehicles,” *IOP Conference Series: Materials Science and Engineering*, vol. 252, p. 012058, 10 2017.
- [3] K. Saqli, H. Bouchareb, M. Oudghiri, and N. M’Sirdi, “Critical review of ageing mechanisms and state of health estimation methods for battery performance,” in *Sustainability in Energy and Buildings. Proceedings of SEB 2019*, ser. Smart Innovation, Systems and Technologies, J. Littlewood, R. J. Howlett, A. Capozzoli, and L. C. Jain, Eds. Springer, 2019, vol. 163, pp. 506–518.
- [4] T. Han, C.-H. Yen, B. Khalighi, and S. Kaushik, “Li-ion battery pack thermal management - liquid vs air cooling,” *Journal of Thermal Science and Engineering Applications*, vol. 11, 09 2018.
- [5] Y. Ye, S. Yixiang, N. Cai, J. Lee, and X. He, “Electro-thermal modeling and experimental validation for lithium ion battery,” *Journal of Power Sources*, vol. 199, p. 227–238, 10 2011.
- [6] N. Yang, X. Zhang, G. Li, and D. Hua, “Assessment of the forced air-cooling performance for cylindrical lithium-ion battery packs: A comparative analysis between aligned and staggered cell arrangements,” *Applied Thermal Engineering*, vol. 80, 04 2015.
- [7] G. Karimi and X. Li, “Thermal management of lithium-ion batteries for electric vehicles,” *International Journal of Energy Research*, vol. 37, 01 2013.
- [8] D. Chen, J. Jiang, G.-H. Kim, C. Yang, and A. Pesaran, “Comparison of different cooling methods for lithium ion battery cells,” *Applied Thermal Engineering*, vol. 94, 10 2015.
- [9] H. Park, “A design of air flow configuration for cooling lithium ion battery in hybrid electric vehicles,” *Journal of Power Sources*, vol. 239, p. 30–36, 10 2013.
- [10] J. Zhao, Z. Rao, H. Yutao, X. Liu, and Y. Li, “Thermal management of cylindrical power battery module for extending the life of new energy electric vehicles,” *Applied Thermal Engineering*, vol. 85, 06 2015.
- [11] Z. Liu, Y. Wang, J. Zhang, and Z. Liu, “Corrigendum to “shortcut computation for the thermal management of a large air-cooled battery pack” [appl. therm. eng. 66 (2014) 445–452],” *Applied Thermal Engineering*, vol. 75, p. 1133, 01 2015.
- [12] M. Chen and G. on Mora, “Accurate electrical battery model capable of predicting runtime and i–v performance,” *IEEE Transactions on Energy Conversion - IEEE TRANS ENERGY CONVERS*, vol. 21, pp. 504–511, 06 2006.
- [13] J. Meng, G. Luo, M. Ricco, M. Swierczynski, D.-I. Stroe, and R. Teodorescu, “Overview of lithium-ion battery modeling methods for state-of-charge estimation in electrical vehicles,” *Applied Sciences*, vol. 8, p. 659, 04 2018.
- [14] M. Doyle, T. F. Fuller, and J. Newman, “Modeling of galvanostatic charge and discharge of the lithium/polymer/insertion cell,” *Journal of The Electrochemical Society*, vol. 140, no. 6, pp. 1526–1533, jun 1993.
- [15] T. F. Fuller, M. Doyle, and J. Newman, “Simulation and optimization of the dual lithium ion insertion cell,” *Journal of The Electrochemical Society*, vol. 141, no. 1, pp. 1–10, jan 1994.
- [16] J. Forman, S. Bashash, J. Stein, and H. Fathy, “Reduction of an electrochemistry-based li-ion battery model via quasi-linearization and padé approximation,” *Journal of The Electrochemical Society*, vol. 158, pp. A93–A101, 02 2011.
- [17] B. Fridholm, T. Wik, and M. Nilsson, “Robust recursive impedance estimation for automotive lithium-ion batteries,” *Journal of Power Sources*, vol. 304, pp. 33–41, 2016.
- [18] R. Zhang, B. Xia, B. Li, L. Cao, Y. Lai, W. Zheng, H. Wang, and W. Wang, “State of the art of lithium-ion battery soc estimation for electrical vehicles,” *Energies*, vol. 11, p. 1820, 07 2018.

#### NOMENCLATURE

##### Subscripts

$e$	electrolyte
$eff$	effective
$max$	maximum
$n$	negative
$p$	positive
$s$	solid
$sep$	separator
$surf$	surface

##### List of symbols

$\epsilon$	porosity
$\eta$	overpotential of the intercalation reaction, V
$\rho$	density, $kg\ m^{-3}$
$\sigma_i$	electronic conductivity of solid matrix, $S\ m^{-1}$
$a_s$	reaction surface area, $m^2\ m^{-3}$
$C_p$	specific heat, $J\ kg^{-1}\ K^{-1}$
$c_s$	concentration of lithium ion in solid, $mol\ m^{-3}$
$D_e$	salt diffusion coefficient, $m^2\ s^{-1}$
$D_s$	diffusion coefficient of lithium ion in solid electrode
$F$	Faraday’s constant, $C\ mol^{-1}$
$J$	pore wall flux of lithium ions, $mol\ m^{-2}\ s^{-1}$
$k_i$	reaction rate, $m^{2.5}\ mol^{-0.5}\ s^{-1}$
$L$	thickness of battery component
$R$	gas constant, $J\ mol^{-1}\ K^{-1}$
$r$	radial coordinate in spherical particle
$T$	temperature, K
$t$	time, s
$t_+$	transference number of lithium ion
$U$	open-circuit potential, V
$x$	spatial coordinate